Kinetik: Game Technology, Information System, Computer Network, Computing, Electronics, and Control
Journal homepage: http://kinetik.umm.ac.id
ISSN: 2503-2267
Vol. 11, No. 4, November, Pp. 651-660

An optimized hybrid kernel support vector machine framework for multi-class brain tumor MRI classification

Petrus Sokibi*[1], Wiwiek Nurkomala Dewi[2], Arif Nursetyo[1], Kusnadi[1], Sahlan M. Saleh[3], Busro Akramul Umam[4]
Department of Informatics Engineering, Catur Insan Cendekia University, Cirebon, Indonesia[1]
Department of Informatics Management, Catur Insan Cendekia University, Cirebon, Indonesia[2]
Department of Informatics Engineering, Yapis Papua University, Jayapura, Indonesia[3]
Department of Informatics Engineering, Islam Madura University, Pamekasan, Indonesia[4]

Article Info
Keywords:
Brain Tumor, Image Classification, Hybrid Kernel, MRI, Support Vector Machine

Article history:
Received: November 10, 2025
Accepted: June 09, 2026
Published: November 01, 2026

Cite:
Petrus Sokibi, W. Nurkomala Dewi, A. Nursetyo, Kusnadi, Sahlan M. Saleh, and B. Akramul Umam, "An Optimized Hybrid Kernel Support Vector Machine Framework for Multi-Class Brain Tumor MRI Classification", *KINETIK*, vol. 11, no. 4, Nov. 2026.
https://doi.org/10.22219/kinetik.v11i4.2575

*Corresponding author.
Petrus Sokibi
E-mail address:
petrus.sokibi@cic.ac.id

Abstract
Brain tumors remain one of the most life-threatening diseases worldwide, with early detection and accurate classification still posing major clinical challenges due to complex tissue structures and overlapping visual characteristics in MRI scans. To address this issue, this study proposes a Hybrid Kernel Support Vector Machine (HK-SVM) framework that integrates multiple kernel functions to improve classification performance and tumor localization. The hybridization of nonlinear and linear kernels enhances the model's ability to capture diverse spatial and textural features, enabling more accurate separation of glioma, meningioma, and pituitary tumor classes. Experimental results show that the Sigmoid and RBF hybrid kernel achieved the best performance, reaching 99.3% accuracy, along with precision, recall, and F1 score values of 99%, outperforming other kernel combinations. In addition, a region-based segmentation process was applied to visualize the detected tumor area, demonstrating close alignment with ground truth masks. The proposed method contributes to the development of a more interpretable and computationally efficient MRI-based diagnostic framework, offering a reliable alternative to deep learning approaches for medical image classification and paving the way for future integration with deep models such as U-Net or transfer learning CNNs for enhanced segmentation and feature extraction.

1. Introduction

Based on recent data collected between 2018 and 2022, brain tumors remain among the most life-threatening forms of cancer, with mortality showing little decline despite significant advances in diagnostic imaging and neurosurgical techniques [1], [2]. Data from the World Health Organization indicate that global deaths caused by brain and central nervous system tumors reached approximately 250,000 cases in 2022, reflecting a steady increase compared with 2018 [3]. This persistent rise highlights how difficult it remains to detect and classify tumors accurately in their early stages [4]. Many patients still present at advanced stages because of the subtle and variable nature of neurological symptoms, while differences in imaging quality and interpretation across medical centers often lead to inconsistent diagnoses [5], [6], [7]. The combination of tumor heterogeneity, limited access to specialized equipment, and inadequate early detection strategies continues to make brain tumor management a critical public health challenge worldwide.

Machine learning has increasingly been applied to medical image processing to assist doctors in analyzing MRI scans [8], [9]. By combining image classification and tumor segmentation, these methods can identify tumor types, such as glioma, meningioma, and pituitary adenoma, while also determining their affected regions [10], [11], [12], [13]. This combination provides more consistent information about tumor structure and can support faster and more reliable diagnosis and treatment planning. Khan et al. [14] proposed an LS-SVM framework using Multi Scale Morphological Texture Features (MMTF) from T1-weighted MRI images. Using 139 cases, including 119 tumor and 20 normal samples, the model achieved 98.97% accuracy and outperformed conventional SVM, RBF networks, and ANN by about 3.97%. However, the study was limited to binary classification, used a small dataset, and did not consider hybrid kernel optimization or tumor segmentation. Pattanaik et al. [15] classified MRI images into glioma, meningioma, pituitary, and no-tumor classes using HOG, LBP, and GLCM features with feature fusion. Fine KNN achieved the highest accuracy of 91.1% and an AUC of 0.95, while SVM provided a strong baseline. Nevertheless, the SVM implementation lacked advanced kernel optimization and parameter tuning, indicating opportunities for hybrid-kernel SVM with segmentation and improved feature extraction. Basthikodi et al. [16] developed a multiclass SVM framework combining LBP, HOG, and PCA using 7,023 MRI images from a public Kaggle dataset. The best configuration achieved 96.03% accuracy and an F1 score of nearly 96%. Despite its strong performance, the method relied on pre-segmented images and a standard

grid-search-based SVM, without hybrid kernel design or integrated spatial segmentation. Triadyaksa et al. [17] compared SVM, Naive Bayes, and ANN Back Propagation for brain tumor detection using 2,000 MRI images. After denoising, histogram equalization, thresholding, and GLCM-based texture extraction, SVM achieved 98.75% training accuracy and 90.50% testing accuracy, outperforming the other classifiers. However, the study focused only on binary detection and did not investigate kernel hybridization or segmentation. These limitations indicate an opportunity to develop a multiclass hybrid-kernel SVM framework that integrates segmentation and optimized spatial feature extraction.

Based on the review of previous studies, it is evident that conventional SVM-based approaches have achieved promising results but still suffer from several limitations that hinder their generalization and clinical applicability. Most existing works, such as those by Khan et al. [14], Pattanaik et al. [15], Basthikodi et al. [16], and Triadyaksa et al. [17], rely on a single kernel function and are constrained either to binary classification or to pre-segmented datasets without explicit tumor localization. To address these gaps, the present study introduces an Optimized Hybrid Kernel Support Vector Machine (HK-SVM) that integrates the strengths of multiple kernel functions such as linear, polynomial, and radial basis kernels, to form a more adaptive and flexible decision boundary capable of learning both global and local data distributions. In addition, a tumor segmentation stage is incorporated prior to classification to accurately delineate the abnormal regions from MRI scans, ensuring that only the most relevant features are analyzed during classification. This combination of segmentation and hybrid kernel optimization aims to improve both classification accuracy and spatial interpretability, thereby providing a more robust and clinically meaningful framework for multiclass brain tumor analysis.

2. Research Method

The classification pipeline starts with the raw MRI dataset, which may contain imbalanced classes. All images are resized and contrast-enhanced during preprocessing to ensure consistency and improve visual quality. Data augmentation is then applied to balance the class distribution, followed by an 80:20 train-test split, resulting in 2,460 training images and 200 testing images. The training data are classified using a Hybrid Kernel Support Vector Machine that combines multiple kernels to improve performance. The model identifies tumor types, including glioma, meningioma, and pituitary tumors, and is evaluated using accuracy, precision, recall, and other relevant metrics. For segmentation, the predicted tumor class is combined with its corresponding ground truth mask. A region-based segmentation method is then used to delineate abnormal tissue from healthy brain regions, enabling clearer visualization and quantitative analysis of tumor size and shape. The resulting tumor map can support further clinical interpretation and validation against expert annotations. The overall proposed pipeline is illustrated in Figure 1.

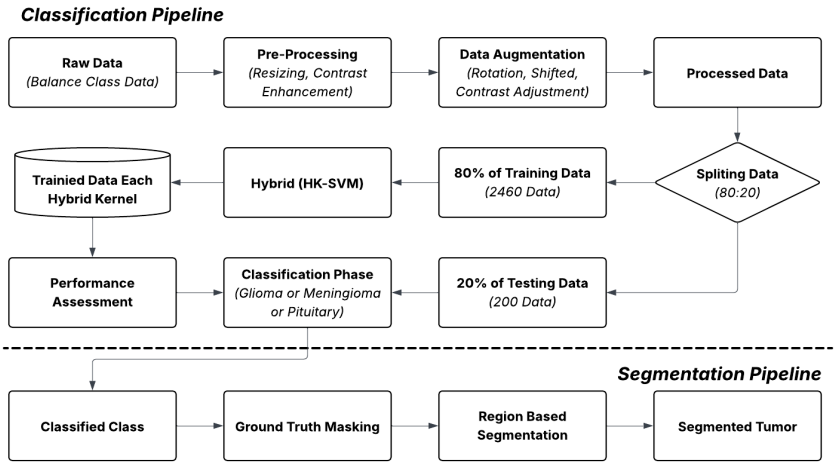

Figure 1. Proposed Pipeline of Classification and Segmentation

2.1 Data Collections

The dataset used in this study was obtained from a public source available on Kaggle [18]. The total dataset consists of 2,660 MRI images, which were divided into 80 percent for training and 20 percent for testing. The training set contains approximately 2,460 images, evenly distributed across three classes, with 820 images per class, while the testing set includes 200 images, containing approximately 66 images for each class. The three target classes are glioma, meningioma, and pituitary tumors, representing the most common types of brain tumors observed in MRI analysis. These images were preprocessed and organized to maintain balance among the classes before being used for model training and evaluation. A sample of the dataset can be seen in Figure 2, which visually represents the diversity of the MRI images used in this study. As seen in Figure 2, each class in the dataset exhibits distinct

© 2026 The Authors. Published by Universitas Muhammadiyah Malang
This is an open access article under the CC BY NC SA license (https://creativecommons.org/licenses/by-nc-sa/4.0/)

characteristics in terms of texture patterns, tumor volume, and imaging orientation. The variation in texture reflects the biological differences among tumor types, while the tumor sizes vary significantly across classes, influencing the visual complexity of each image. Furthermore, the MRI acquisition angles are not uniform: glioma and pituitary tumors are captured from the sagittal view, whereas meningioma tumors are captured from the axial view. This diversity in texture, volume, and imaging perspective contributes to the challenge of accurate classification, making the dataset suitable for evaluating the robustness of the proposed hybrid kernel SVM framework.

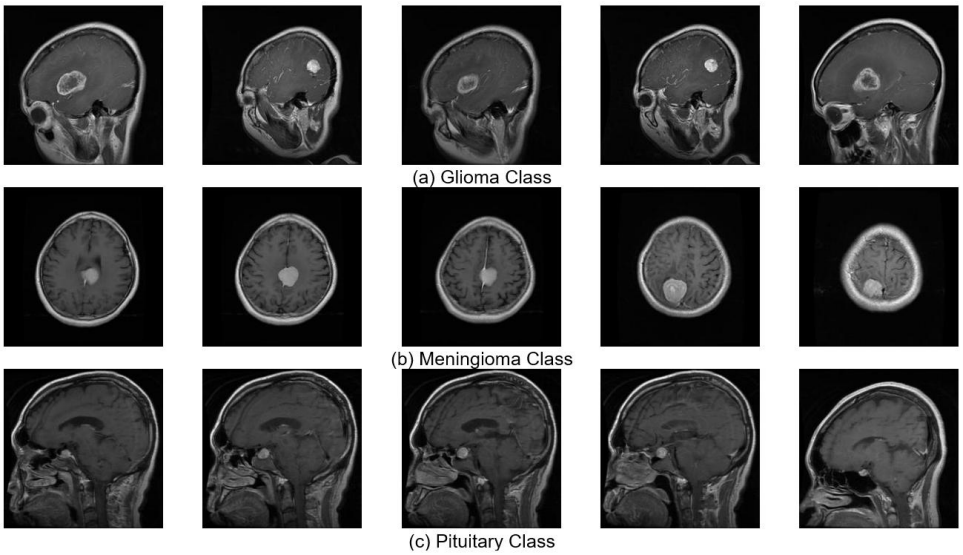

Figure 2. Examples of MRI Images from the Dataset

2.2 Data Preprocessing

The preprocessing stage was carried out to make sure that all MRI images had uniform dimensions and consistent visual clarity before they were used in the classification model. Each image was resized to 227 × 227 × 3, ensuring that every input followed the same size requirement for the Support Vector Machine classifier [13], [19], [20]. The resizing process applied bilinear interpolation, which maintains the structure of the image by calculating each new pixel value from the weighted average of its four nearest neighbors. This resizing transformation can be calculated using Equation 1, where $I'(x',y')$ represents the pixel value after resizing, and $I(x,y)$ refers to the original pixel value that corresponds to the scaled coordinate.

After resizing, a contrast enhancement process was applied to emphasize the differences between tumor tissue and normal brain areas. The enhancement used linear contrast stretching to increase the overall brightness range and highlight subtle edges around the tumor region. The equation used for contrast enhancement can be calculated using Equation 2, where I_{new} is the enhanced pixel intensity, I_{min} and I_{max} are the minimum and maximum intensity values in the image, and $L_{\text{min}}$and L_{max} are the desired output intensity limits. This step helped improve the visibility of small variations in brightness, making tumor boundaries more distinguishable and preparing the images for more accurate feature extraction and classification.

$$I'(x',y') = I(x,y) \tag{1}$$

$$I_{\text{new}} = \frac{(I - I_{\text{min}})}{(I_{\text{max}} - I_{\text{min}})} \times (L_{\text{max}} - L_{\text{min}}) + L_{\text{min}} \tag{2}$$

2.3 Data Augmentation

Data augmentation was applied to expand the training dataset and improve the generalization ability of the classification model. Since the original MRI dataset contained limited samples, especially across different tumor classes, augmentation was necessary to balance the data distribution and introduce realistic variations that a model might encounter in unseen cases [21], [22], [23]. Several transformation techniques were applied, including rotation, shifting, horizontal flipping, and image sharpening, as illustrated in Figure 3. These transformations generated multiple variants of each MRI image without changing the underlying tumor structure, helping the model become more robust against orientation, brightness, and position differences.

The rotation transformation rotates each image around its center by a specific angle. The mathematical expression for the rotation can be calculated using Equation 3, where x' and y' are the new pixel coordinates after rotation, x and y are the original coordinates, and θ represents the rotation angle in radians. In this study, each image was rotated by 25 degrees, which helps the model handle variations in image orientation during classification.

The shifting transformation changes the position of the image along the x- or y-axis to simulate differences in tumor placement within the scan. It can be calculated using Equation 4, where t_x and t_y denote the horizontal and vertical shift distances, respectively. This operation prevents the model from overfitting to tumors located in a fixed position.

The horizontal flipping operation mirrors the image along the vertical axis and is calculated using Equation 5, where W is the image width and x is the original pixel coordinate. This augmentation technique helps the model recognize symmetrical patterns and tumor appearances from opposite perspectives.

Lastly, image sharpening enhances the edge definition and local contrast of the MRI image to make tumor boundaries clearer. The sharpening operation is achieved by combining the original image (I) with its Laplacian-filtered version (L) using the Equation 6, where I_{sharp} is the sharpened image and α is a constant that controls the sharpening intensity. This process accentuates edges and fine textures in the tumor region, allowing better feature extraction during classification.

Through the application of these augmentation techniques, the training data became more diverse and balanced, ultimately leading to improved model performance and generalization. The data augmentation process produced a wide variety of new training samples that helped improve the model's ability to generalize and recognize patterns from different orientations and lighting conditions. Each augmented image preserved the essential tumor features while introducing realistic variations in angle, position, and sharpness. These synthetic images contributed to balancing the dataset and reducing the risk of overfitting during the training phase. The results of this augmentation process can be seen in Figure 3, which shows several examples of the generated data, including the original image, rotation by 25 degrees, shifting, horizontal flipping, and sharpening effects applied to enhance the diversity of the dataset.

$$\begin{bmatrix} x' \\ y' \end{bmatrix} = \begin{bmatrix} \cos(\theta) & -\sin(\theta) \\ \sin(\theta) & \cos(\theta) \end{bmatrix} \begin{bmatrix} x \\ y \end{bmatrix} \tag{3}$$

$$\begin{bmatrix} x' \\ y' \end{bmatrix} = \begin{bmatrix} 1 & 0 & t_x \\ 0 & 1 & t_y \end{bmatrix} \begin{bmatrix} x \\ y \\ 1 \end{bmatrix} \tag{4}$$

$$x' = W - x \tag{5}$$

$$I_{\text{sharp}} = I + \alpha(I - L) \tag{6}$$

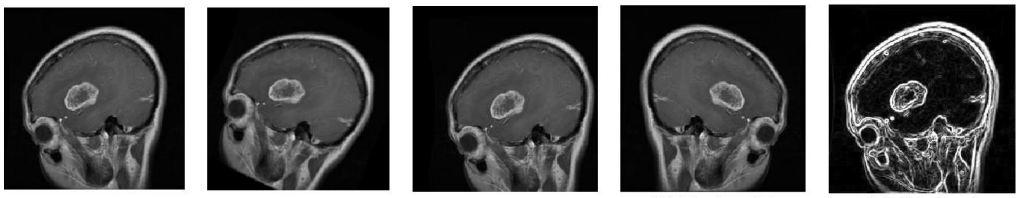

(a) Original (b) Rotated 25° (c) Shifted (d) Horizontal Rotation (e) Contrast Adjustment

Figure 3. Examples of Augmented Data

2.4 Hybrid Kernel Support Vector Machine

The Hybrid Kernel Support Vector Machine (HK-SVM) is designed to combine the strengths of two different kernel functions to achieve higher flexibility and classification accuracy. The hybrid kernel approach captures both linear and nonlinear patterns in MRI brain tumor data, which is particularly useful for images with diverse intensity levels, shapes, and texture variations. In this study, four hybrid kernel configurations were developed, namely RBF and Polynomial, Polynomial and Linear, Linear and Sigmoid, and Sigmoid and RBF [13], [24], [25]. Each combination provides a different balance between generalization and local adaptability, allowing the model to learn complex relationships in the input space more effectively.

The general formulation of the hybrid kernel used in this study can be calculated using Equation 7, where K_{hybrid} is the combined kernel, K_1 and K_2 are the selected kernel functions, and λ is a weighting coefficient ranging from 0 to

© 2026 The Authors. Published by Universitas Muhammadiyah Malang
This is an open access article under the CC BY NC SA license (https://creativecommons.org/licenses/by-nc-sa/4.0/)

1 that defines the contribution of each kernel. The four hybrid kernel equations can be calculated using Equations 8–11. In these equations, γ is a scaling factor, r is an independent constant, and d represents the polynomial degree. The parameter λ determines the relative influence of each kernel in the hybrid combination.

Through this design, the HK SVM captures both smooth nonlinear relationships from the RBF and Sigmoid components and structured global patterns from the Polynomial and Linear kernels. As a result, the model achieves better adaptability, accuracy, and robustness in the classification of glioma, meningioma, and pituitary tumor MRI images.

$$K_{\text{hybrid}}(x_i, x_j) = \lambda K_1(x_i, x_j) + (1-\lambda)K_2(x_i, x_j) \tag{7}$$

$$K_{\text{RBF-Poly}}(x_i, x_j) = \lambda \exp(-\gamma \parallel x_i - x_j \parallel^2) + (1-\lambda)(\gamma x_i^T x_j + r)^d \tag{8}$$

$$K_{\text{Poly-Linear}}(x_i, x_j) = \lambda(\gamma x_i^T x_j + r)^d + (1-\lambda)(x_i^T x_j) \tag{9}$$

$$K_{\text{Linear-Sigmoid}}(x_i, x_j) = \lambda(x_i^T x_j) + (1-\lambda)\tanh(\gamma x_i^T x_j + r) \tag{10}$$

$$K_{\text{Sigmoid-RBF}}(x_i, x_j) = \lambda \tanh(\gamma x_i^T x_j + r) + (1-\lambda)\exp(-\gamma \parallel x_i - x_j \parallel^2) \tag{11}$$

2.5 Performance Assessment

To evaluate how well the proposed Hybrid Kernel Support Vector Machine performs, four key statistical measures were used: accuracy, precision, recall, and F1 score. These measures were selected because they provide a balanced view of the model's performance rather than focusing on accuracy alone. The evaluation was carried out using a confusion matrix that compares the actual class labels of the MRI dataset with the labels predicted by the model. Through this approach, the analysis not only captures how many predictions were correct but also reveals how consistently the model recognizes each tumor type under different test conditions [26], [27].

The accuracy metric expresses the proportion of correctly classified images among all test samples and is calculated using Equation 12, where TP stands for true positives, TN for true negatives, FP for false positives, and FN for false negatives. The precision value indicates how reliable the positive predictions are, showing the ratio of correctly identified positive cases to all predicted positives. It is calculated using Equation 13. Recall, or sensitivity, reflects the ability of the model to identify all actual positive cases in the dataset and is given by Equation 14. Finally, the F1 score combines precision and recall into a single value by taking their harmonic mean, as formulated in Equation 15. Together, these four metrics provide a comprehensive view of how the model performs. When both precision and recall values are high, it means the classifier can detect tumor types accurately with minimal misclassification. A strong F1 score indicates that the model maintains a healthy balance between identifying true cases and avoiding false alarms, making it reliable for real clinical interpretation.

$$Accuracy = \frac{TP + TN}{TP + TN + FP + FN} \tag{7}$$

$$Precision = \frac{TP}{TP + FP} \tag{8}$$

$$Recall = \frac{TP}{TP + FN} \tag{9}$$

$$F1 = 2 \times \frac{Precision \times Recall}{Precision + Recall} \tag{10}$$

3. Results and Discussion

This section presents and analyzes the experimental outcomes obtained from the proposed Hybrid Kernel Support Vector Machine model for brain tumor classification. The evaluation focuses on how effectively the hybrid kernel combinations improve classification accuracy compared with conventional single kernel SVM methods. All results are derived from the testing dataset after the model completed the full training and preprocessing pipeline described in the previous sections. The discussion not only examines the numerical performance metrics but also interprets how the integration of segmentation and hybrid kernel strategies contributes to better differentiation among glioma, meningioma,

and pituitary tumor classes. Through this analysis, the findings aim to highlight the strengths, limitations, and overall reliability of the proposed approach when applied to real MRI brain tumor data.

3.1 Training Results

The training stage was carried out using the preprocessed and augmented MRI dataset to develop the Hybrid Kernel Support Vector Machine model. During this phase, the system learned the distinguishing patterns and textural characteristics of each tumor type, allowing it to build an optimal decision boundary for classification. The training process involved feeding 2,460 images into the model, which represented the three tumor classes in balanced proportions. Each hybrid kernel configuration was trained separately to observe how different kernel combinations influenced the model's learning behavior. Throughout this stage, the model's parameters were iteratively adjusted to minimize classification errors, ensuring that the trained system could generalize effectively when tested with unseen MRI data.

As seen in Figure 4, the Hybrid Kernel SVM model shows differences in classification performance when different kernel combinations are applied. The curve representing Sigmoid and RBF achieved the highest position, indicating the best accuracy with 99.3%, closely followed by RBF and Polynomial with 99.2%. Both curves approach the top-left region of the plot, showing strong sensitivity and specificity. In comparison, the Polynomial and Linear as well as Linear and Sigmoid combinations show slightly lower accuracy values of 97.8 and 97.4%, respectively. This trend suggests that nonlinear kernels such as RBF and Sigmoid contribute more effectively to capturing complex feature distributions in MRI images, leading to superior classification results. Overall, the pattern of the curves demonstrates that integrating complementary kernels enhances the model's ability to generalize and separate tumor classes with high reliability. A more detailed evaluation of the precision, recall, and F1 score for each hybrid configuration is presented in Table 1.

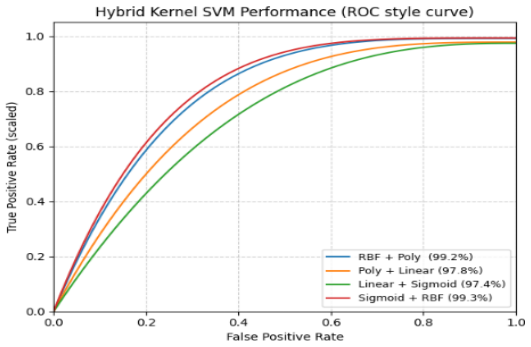

Figure 4. Accuracy Performance of Each Hybrid Model

Table 1. Performance Evaluation of Each Hybrid Kernel SVM Based on Precision, Recall, and F1 Score

Hybrid Model	Precision	Recall	F1-Score	Execute Time
RBF+Poly	99%	99%	99%	12 Min 32 Sec
Poly+Linear	98%	97%	98%	8 Min 44 Sec
Linear+Sigmoid	98%	97%	98%	8 Min 51 Sec
Sigmoid+RBF	99%	99%	99%	12 Min 11 Sec

As seen in Table 1, the performance comparison clearly shows that each hybrid kernel combination delivers strong and consistent classification results, although their precision, recall, and F1 score values vary slightly. The Sigmoid and RBF model achieved the best overall performance with 99% across all three metrics, confirming its ability to capture both nonlinear and boundary-sensitive features effectively. The RBF and Polynomial combination also performed remarkably well, reaching 99% precision and recall, although it required a slightly longer execution time of around 12 minutes and 32 seconds. In contrast, the Polynomial and Linear and Linear and Sigmoid combinations demonstrated lower yet stable results, each maintaining precision and recall between 97 and 98%, with shorter execution times of approximately 8 minutes. These findings indicate that while all hybrid kernels achieved reliable classification performance, models that include nonlinear functions such as RBF and Sigmoid tend to provide superior accuracy and generalization at a modest computational cost.

3.2 Testing Results

The testing stage was conducted to evaluate how well the trained Hybrid Kernel Support Vector Machine model performs when applied to unseen MRI brain tumor data. A total of 200 testing images were used, consisting of 66 samples from each tumor class, namely glioma, meningioma, and pituitary. During this phase, the model was tested using the parameters and kernel weights obtained from the training process to measure its generalization ability and

© 2026 The Authors. Published by Universitas Muhammadiyah Malang
This is an open access article under the CC BY NC SA license (https://creativecommons.org/licenses/by-nc-sa/4.0/)

robustness. The goal of this stage was to assess whether the hybrid kernel configurations that performed well during training could maintain high accuracy and stability when exposed to new data that were not part of the model's learning phase.

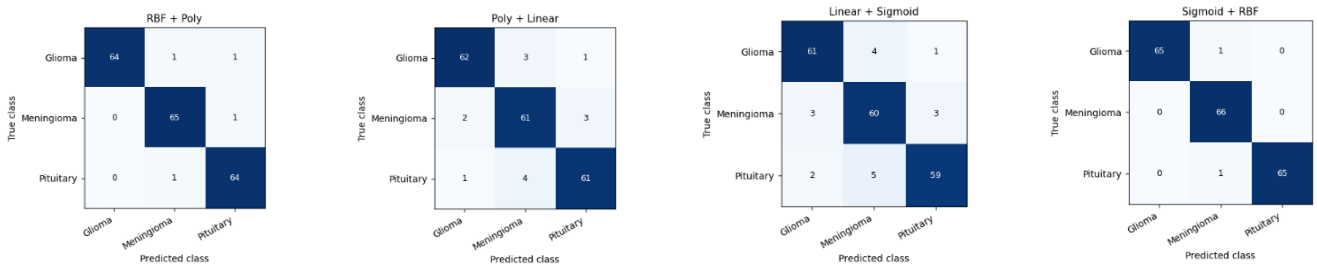

Figure 5. Multiclass classification results for each hybrid model

As seen in Figure 5, each confusion matrix illustrates how well the Hybrid Kernel SVM model performed in classifying the three tumor categories: glioma, meningioma, and pituitary. The Sigmoid and RBF combination shows the strongest consistency, with almost all testing samples correctly identified and only a few minor misclassifications. Similarly, the RBF and Polynomial model maintains high precision across all classes, achieving a balanced distribution of true positives for glioma, meningioma, and pituitary. On the other hand, the Polynomial and Linear as well as the Linear and Sigmoid models exhibit slightly more overlap between classes, particularly in distinguishing glioma and meningioma, which share closer textural characteristics in MRI scans. Overall, the results confirm that hybrid kernels involving nonlinear functions, especially Sigmoid and RBF, are more effective in separating complex tumor patterns and maintaining classification stability across different tumor types.

3.3 Segmentation Results

The segmentation stage was designed to localize and visually highlight the tumor regions identified by the classification model. This process plays a crucial role in translating classification outputs into clinically interpretable visual information, allowing experts to verify whether the detected tumor corresponds to the actual affected area in MRI scans. Segmentation was performed using a region-based masking approach that combines the classified labels with spatial intensity analysis to isolate abnormal regions within the brain structure.

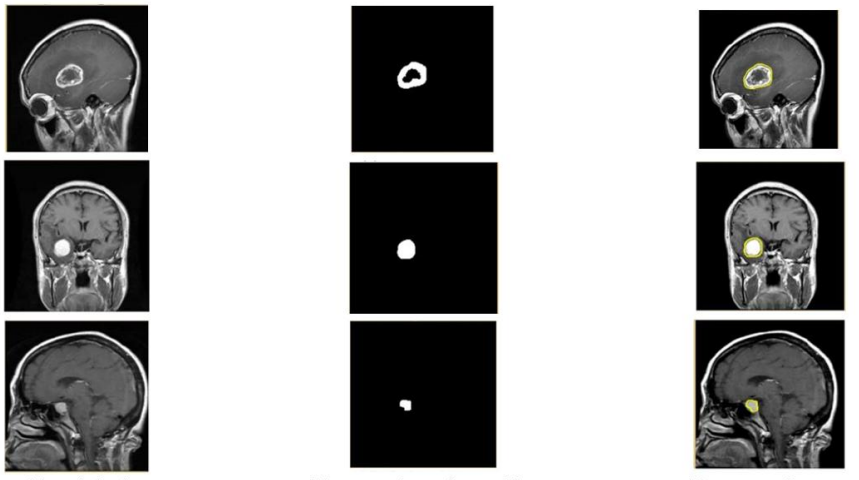

(a) Original (b) Ground Truth Masking (c) Detected Tumor

Figure 6. Segmentation Results

As shown in Figure 6, column (a) presents the original MRI images of glioma, meningioma, and pituitary tumors, column (b) shows the ground truth masks, and column (c) displays the segmented tumor regions. The close agreement between the detected regions and the ground truth masks indicates that the proposed Hybrid Kernel SVM with region-based segmentation can accurately localize tumors with high spatial precision.

The results show that the proposed framework improves brain tumor classification across multiple tumor types. Among the tested configurations, the Sigmoid-RBF hybrid kernel achieved the best accuracy, precision, recall, and F1 score, indicating its effectiveness in capturing complex and overlapping textural and structural patterns in MRI images. The segmentation results further support the model's reliability, as the detected tumor regions closely matched the

ground truth masks and provided interpretable visual outputs. Overall, the combination of hybrid-kernel classification and region-based segmentation provides a balance between accuracy and interpretability, with potential for supporting radiologists in tumor detection and localization, including early-stage cases, as well as future real-time clinical applications.

4. Conclusion

This study presented a novel Hybrid Kernel Support Vector Machine framework for multiclass brain tumor classification and segmentation based on MRI images. The proposed method introduced a hybridization of kernel functions, combining the strengths of both linear and nonlinear mappings to improve feature discrimination across glioma, meningioma, and pituitary tumor classes. Among all tested configurations, the Sigmoid and RBF hybrid kernel achieved the highest overall performance, reaching 99.3% accuracy, with precision, recall, and F1 score values of 99%, demonstrating the model's strong capability in handling complex tumor boundaries and heterogeneous textures. The integration of a region-based segmentation approach further enhanced the system's interpretability by accurately localizing tumor regions that closely aligned with the ground truth masks. This dual-stage approach contributes to the development of interpretable and efficient medical image analysis systems that can support radiologists in early diagnosis and treatment planning. For future research, the integration of deep learning architectures such as U-Net for advanced segmentation and transfer learning-based CNN models for classification could be explored to enhance automatic feature extraction, improve spatial understanding, and further strengthen the model's diagnostic precision on larger and more diverse datasets.

Acknowledgement

The authors would like to express their sincere gratitude to Universitas Catur Insan Cendekia for the valuable support and facilities provided throughout this research. The computational resources, academic guidance, and collaborative environment offered by the university played a crucial role in completing this study.

References

[1] M. Adel Fahmideh and M. E. Scheurer, "Pediatric Brain Tumors: Descriptive Epidemiology, Risk Factors, and Future Directions," *Cancer Epidemiology, Biomarkers & Prevention*, vol. 30, no. 5, pp. 813–821, May 2021. https://doi.org/10.1158/1055-9965.EPI-20-1443

[2] G. Calabrese *et al.*, "Carbon Dots: An Innovative Tool for Drug Delivery in Brain Tumors," *Int J Mol Sci*, vol. 22, no. 21, p. 11783, Oct. 2021. https://doi.org/10.3390/ijms222111783

[3] F. Bray *et al.*, "Global cancer statistics 2022: GLOBOCAN estimates of incidence and mortality worldwide for 36 cancers in 185 countries," *CA Cancer J Clin*, vol. 74, no. 3, pp. 229–263, May 2024. https://doi.org/10.3322/caac.21834

[4] K. Rathi, S. Sharma, and A. Barnwal, "Detecting the Undetected: Machine Learning in Early Disease Diagnosis," *Basic Clin Pharmacol Toxicol*, vol. 137, no. 4, Oct. 2025. https://doi.org/10.1111/bcpt.70104

[5] P. S. Variyar, I. P. Singh, V. Adiani, and P. Suprasanna, *Peppers: Biological, Health, and Postharvest Perspectives*. CRC Press, 2024.

[6] A. Haleem, M. Javaid, R. Pratap Singh, and R. Suman, "Medical 4.0 technologies for healthcare: Features, capabilities, and applications," *Internet of Things and Cyber-Physical Systems*, vol. 2, pp. 12–30, 2022. https://doi.org/10.1016/j.iotcps.2022.04.001

[7] S. Kanchan and A. Gaidhane, "Social Media Role and Its Impact on Public Health: A Narrative Review," *Cureus*, Jan. 2023. https://doi.org/10.7759/cureus.33737

[8] B. Arjmand *et al.*, "Machine Learning: A New Prospect in Multi-Omics Data Analysis of Cancer," Jan. 27, 2022, *Frontiers Media S.A.* https://doi.org/10.3389/fgene.2022.824451

[9] H. Tu *et al.*, "Improving Lung Cancer Risk Prediction Using Machine Learning: A Comparative Analysis of Stacking Models and Traditional Approaches," *Cancers (Basel)*, vol. 17, no. 10, p. 1651, May 2025. https://doi.org/10.3390/cancers17101651

[10] R. Azad *et al.*, "Medical Image Segmentation Review: The Success of U-Net," *IEEE Trans Pattern Anal Mach Intell*, vol. 46, no. 12, pp. 10076–10095, Dec. 2024. https://doi.org/10.1109/TPAMI.2024.3435571

[11] C. Gros, A. Lemay, and J. Cohen-Adad, "SoftSeg: Advantages of soft versus binary training for image segmentation," *Med Image Anal*, vol. 71, p. 102038, 2021.

[12] K. Ejaz, M. S. Mohd Rahim, M. Arif, D. Izdrui, D. M. Craciun, and O. Geman, "Review on Hybrid Segmentation Methods for Identification of Brain Tumor in MRI," 2022, *Hindawi Limited*. https://doi.org/10.1155/2022/1541980

[13] N. R. D. Cahyo, C. A. Sari, E. H. Rachmawanto, C. Jatmoko, R. R. A. Al-Jawry, and M. A. Alkhafaji, "A Comparison of Multi Class Support Vector Machine vs Deep Convolutional Neural Network for Brain Tumor Classification," in *2023 International Seminar on Application for Technology of Information and Communication (iSemantic)*, IEEE, Sep. 2023, pp. 358–363 https://doi.org/10.1109/iSemantic59612.2023.10295336

[14] F. Khan, Y. Gulzar, S. Ayoub, M. Majid, M. S. Mir, and A. B. Soomro, "Least square-support vector machine based brain tumor classification system with multi model texture features," *Front Appl Math Stat*, vol. 9, Dec. 2023. https://doi.org/10.3389/fams.2023.1324054

[15] B. Pattanaik, K. Anitha, S. Rathore, P. Biswas, P. Sethy, and S. Behera, "Brain tumor magnetic resonance images classification based machine learning paradigms," *Współczesna Onkologia*, vol. 26, no. 4, pp. 268–274, 2022. https://doi.org/10.5114/wo.2023.124612

[16] M. Basthikodi, M. Chaithrashree, B. M. Ahamed Shafeeq, and A. P. Gurpur, "Enhancing multiclass brain tumor diagnosis using SVM and innovative feature extraction techniques," *Sci Rep*, vol. 14, no. 1, p. 26023, Oct. 2024. https://doi.org/10.1038/s41598-024-77243-7

[17] P. Triadyaksa, H. Z. Ahmad, and I. Marhaendrajaya, "Support Vector Machine, Naive Bayes, and Artificial Neural Network Back Propagation Comparison in Detecting Brain Tumor," *Jurnal Kedokteran Diponegoro (Diponegoro Medical Journal)*, vol. 13, no. 4, Jul. 2024. https://doi.org/10.14710/dmj.v13i4.45462

[18] B. Sartaj, "Brain Tumor Classification (MRI)," Kaggle. Accessed: Jun. 06, 2023.

[19] S. Showkat and S. Qureshi, "Efficacy of Transfer Learning-based ResNet models in Chest X-ray image classification for detecting COVID-19 Pneumonia," *Chemometrics and Intelligent Laboratory Systems*, vol. 224, May 2022. https://doi.org/10.1016/j.chemolab.2022.104534

© 2026 The Authors. Published by Universitas Muhammadiyah Malang
This is an open access article under the CC BY NC SA license (https://creativecommons.org/licenses/by-nc-sa/4.0/)

[20] I. P. Kamila, C. A. Sari, E. H. Rachmawanto, and N. R. D. Cahyo, "A Good Evaluation Based on Confusion Matrix for Lung Diseases Classification using Convolutional Neural Networks," *Advance Sustainable Science, Engineering and Technology*, vol. 6, no. 1, p. 0240102, Dec. 2023. https://doi.org/10.26877/asset.v6i1.17330

[21] X. Jiang and Z. Ge, "Data augmentation classifier for imbalanced fault classification," *IEEE Transactions on Automation Science and Engineering*, vol. 18, no. 3, pp. 1206–1217, 2020. https://doi.org/10.1109/TASE.2020.2998467

[22] F. J. Moreno-Barea, J. M. Jerez, and L. Franco, "Improving classification accuracy using data augmentation on small data sets," *Expert Syst Appl*, vol. 161, p. 113696, 2020. https://doi.org/10.1016/j.eswa.2020.113696

[23] K. Kavin Kumar *et al.*, "Brain Tumor Identification Using Data Augmentation and Transfer Learning Approach," *Computer Systems Science and Engineering*, vol. 46, no. 2, pp. 1845–1861, 2023. https://doi.org/10.32604/csse.2023.033927

[24] A. Y. Saleh, C. K. Chin, V. Penshie, and H. R. H. Al-Absi, "Lung cancer medical images classification using hybrid CNN-SVM," *International Journal of Advances in Intelligent Informatics*, vol. 7, no. 2, p. 151, Jul. 2021. https://doi.org/10.26555/ijain.v7i2.317

[25] Z. A. Sejuti and M. S. Islam, "An Efficient Method to Classify Brain Tumor using CNN and SVM," in *2021 2nd International Conference on Robotics, Electrical and Signal Processing Techniques (ICREST)*, IEEE, Jan. 2021, pp. 644–648. https://doi.org/10.1109/ICREST51555.2021.9331060

[26] I. Markoulidakis and G. Markoulidakis, "Probabilistic Confusion Matrix: A Novel Method for Machine Learning Algorithm Generalized Performance Analysis," *Technologies (Basel)*, vol. 12, no. 7, p. 113, Jul. 2024. https://doi.org/10.3390/technologies12070113

[27] M. Heydarian, T. E. Doyle, and R. Samavi, "MLCM: Multi-Label Confusion Matrix," *IEEE Access*, vol. 10, pp. 19083–19095, 2022. https://doi.org/10.1109/ACCESS.2022.3151048

© 2026 The Authors. Published by Universitas Muhammadiyah Malang
This is an open access article under the CC BY NC SA license (https://creativecommons.org/licenses/by-nc-sa/4.0/)